


RESEARCH

Open Access



# Effect of tip clearance on non-synchronous propagating flow disturbances of compressor rotors under high aerodynamic loading conditions

Songbai Wang<sup>1,2\*</sup> , Yong Chen<sup>1</sup> and Yadong Wu<sup>1</sup>

\*Correspondence:  
wsb\_buaa@163.com

<sup>1</sup> School of Mechanical Engineering, Shanghai Jiao Tong University, Shanghai 200240, China

<sup>2</sup> AECC Sichuan Gas Turbine Establishment, Chengdu 610500, China

## Abstract

The complex tip flow instability and its induced non-synchronous vibration have become significant challenges, especially as aerodynamic loading continues to increase. This study investigates the effects of tip clearance on non-synchronous propagating flow disturbances of compressor rotors under high aerodynamic loading conditions by conducting full-annulus unsteady numerical simulations with three typical tip clearance values for a 1-1/2 stage transonic compressor. The non-synchronous aerodynamic excitation frequency, circumferential mode characteristics, and annular unstable flow structures are analyzed under near stall conditions. The results show that the total pressure ratio and normalized mass flow parameters first increase and then decrease as the tip clearance increases from 0.5%C (where C represents the tip chord length) to 2%C under high aerodynamic loading conditions, instead of constantly decreasing. For the 0.5%C tip clearance case, the traveling large-scale tornado-like separation vortices cause a low non-synchronous aerodynamic excitation frequency and severe pressure fluctuations. The periodic shedding and reattachment processes of the rotor blades separated by 2 – 3 pitches result in 19 dominant mode orders in the circumferential direction. As the tip clearance increases from 1%C to 2%C, the difference of tip flow structures in each blade passage is significantly weakened, and the dominant mode order of the disturbance is equal to the rotor blade-passing number. The pressure fluctuation is mainly caused by cross-channel tip leakage flow, and the aerodynamic excitation frequency exhibits evident broadband hump characteristics, which has been reported as a rotating instability phenomenon.

**Keywords:** Non-synchronous aerodynamic excitation, Transonic axial compressor, Tip clearance, Unstable flow, Computational Fluid Dynamics

## 1 Introduction

The axial compressor is the core component of an aeroengine. As the aerodynamic stage loading of the compressor continues to increase, rotor blades are more susceptible to suffering the flow-induced vibration problems. In recent years, a new type of flow-induced vibration, non-synchronous vibration (NSV), has been reported by many

scholars [1–5]. Non-synchronous aerodynamic excitation is characterized by a nonintegral multiple of the rotating frequency, and it occurs in the off-design operating region. The significant vibration stress generated by the NSV poses a serious threat to the high-cycle fatigue of rotor blades.

Non-synchronous aerodynamic excitations usually pose a remarkable aeroelastic problem, and the physical mechanism behind them is not fully understood. Previous studies suggested that the occurrence of NSV is closely related to the unstable flow in the rotor tip region [6, 7]. Mailach et al. [8–10] conducted a low-speed axial compressor experiment on the rotating instability phenomenon; they found that rotating instability was observed at both 3% and 4.3% large tip clearances. This instability is characterized by a high-energy hump spectrum below the blade-passing frequency, which includes a set of higher-order modes than rotating stall. The primary mode is approximately half the number of rotor blades, and the circumferential propagation speed is approximately 50% of the rotating speed. Im et al. [11, 12] investigated the aerodynamic excitation mechanism of rotor tip flow instabilities. The results showed that the size and shape of the tip clearance had a significant effect on the frequency and amplitude of the NSV and that the tornado-like tip vortex oscillating along the flow direction was the main cause of the NSV. Tip clearance has a significant impact on the development of tip leakage and unstable flows. Wu et al. [13] studied the frequency and modal characteristics of rotational instability for four different tip clearances. For large tip clearances, the leading edge and leakage vortices combine into a passage vortex, which propagates to the leading edge of the next blade and breaks into two parts: a leading edge vortex and a tip leakage vortex. The flow intensity weakened as the tip clearance decreased, the main mode increased, and the fluctuation intensity and circumferential propagation of the passage vortices were closely related to the intensity of the rotating instability.

In addition to the influence of the tip flow instability, the tip clearance can affect the flow-induced vibration of the rotor blades. Peng [14] investigated the effects of a large tip running clearance on a flutter boundary, and the results showed that compressors with large rotor tip clearances are susceptible to tip unstable flow-induced flutter instability, and that small changes in variable stator vane mal-schedules or negative incidence can offset the oscillating vortices. Jüngst et al. [15] conducted an experimental study on a Darmstadt transonic compressor with a rotor setup with a large tip clearance of 2.5% chord. Pressure fluctuations occurred owing to the rotating instability of the tip circumferential region, where the vortex excited the blade when the frequency matched, and the aerodynamic modes and structural nodal diameter synchronized. Han et al. [16, 17] used forced blade motion to study the relationship between the tip leakage flow and the blade locking frequency. The results indicated that the frequency-locking phenomenon requires the frequency of the tip leakage flow to be sufficiently close to the blade vibration frequency. When the frequency difference between the tip leakage flow and the vibration frequency is less than 1% – 1.6%, the frequency-locking phenomenon may occur, and the bending mode has a greater impact on the stability of the tip leakage flow than the torsional mode. Drolet et al. [18] investigated the effect of the operating temperature and tip clearance size on the tip instability coefficient to predict the critical NSV speed and found that the tip leakage flow can act as an impinging resonant jet on the rotor blades at high aerodynamic loading near the stall.

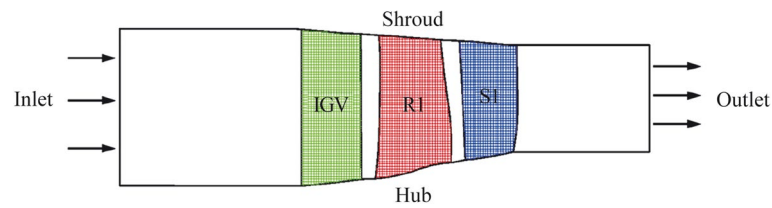


**Fig. 1** Meridian profile of the 1-1/2 stage compressor

**Table 1** Design parameters of the compressor

Parameters	Detail
Blade number (IGV/R1/S1)	52/47/68
Rotor blade profile	Transonic airfoil
Rotor aspect ratio	1.48
Hub-tip ratio	0.74
Dimensionless tip clearance	0.5%
Design physical speed	13,300 rpm
Chord length of rotor tip	57.4 mm

This research indicates that there is an important relationship between the NSV and the instability of the tip flow. These studies tend to investigate the effect of tip leakage flow on the NSV, but what is the physical mechanism by which changes in tip clearance affect the non-synchronous propagating flow disturbances and the aerodynamic excitation frequency characteristics of the unstable flow for different tip clearances? Neither of these questions were answered in a previous study. In this study, the effect of tip clearance on the non-synchronous aerodynamic propagating flow disturbances of transonic compressor rotors under high aerodynamic loading conditions was investigated. This study aims to explore the flow mechanism and aerodynamic excitation frequency characteristics owing to the tip clearance variations.

## 2 Geometry and numerical methods

### 2.1 Research object

A 1-1/2 stage high-speed axial compressor was used as the research object in this study; the meridian profile of the 1-1/2 stage compressor is shown in Fig. 1. The compressor consists of 52 inlet guide vanes, 47 rotor blades, and 68 stator blades. The tip clearance of the rotor blade was approximately 0.5% of its tip axial chord, the chord length of the rotor blade was approximately 57.4 mm, and the rotor aspect ratio was 1.48. The primary design parameters of the compressor are listed in Table 1.

### 2.2 Computational mesh and boundary conditions

An O4H-type structure fluid grid was adopted in every row. The full-annulus computational grid and detailed views are shown in Fig. 2. To capture the leakage flow, the tip clearance mesh was refined to 17 layers in the radial direction. The  $y^+$  in the first inner cell was approximately 15 – 25, which is appropriate for the  $k-\varepsilon$  turbulence model. Many scholars have adopted this turbulence model to study the mechanism of

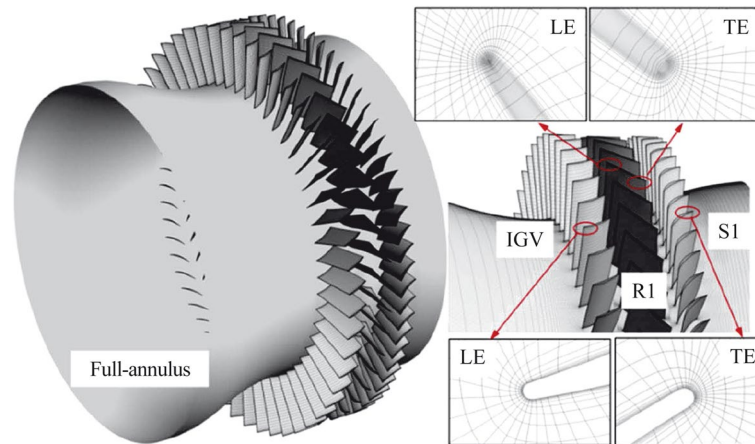


**Fig. 2** Computational grid and detailed views

**Table 2** Four sets of grids with different dimensions

Grid number	Single channel model ( $\times 10^4$ )	Full-annulus model ( $\times 10^4$ )
Grid 1	65	3500
Grid 2	110	6200
Grid 3	154	8300
Grid 4	195	10400

flow instability in axial compressors [19, 20]. The total mesh size for the full-annulus simulation of 1-1/2 stage compressor stages was approximately 62 million nodes.

The sensitivity of the grid-independent test was processed under four grid levels, and the four sets of grids with different dimensions are listed in Table 2. Considering the high computational cost of full-annulus unsteady numerical simulations, the grid independence was verified using steady calculations of single-channel models. A comparison of the total pressure ratio parameters is shown in Fig. 3, where the total pressure ratio parameter tends to stabilize as the grid number increases. The variation in the total pressure ratio for Grids 1 and 2 was approximately 0.24%, the variation from Grids 2 to 4 was within 0.03%, and the refinement of Grids 2 to 3 did not result in substantial changes to the numerical results. Grid 2 was selected as the scheme for the unsteady numerical simulation of a 1-1/2 stage compressor considering CPU time consumption.

In the unsteady simulation, the physical time step consisted of 32 time steps for each rotor blade-passing period, accompanied by 10 inner iterations. The inlet boundary condition was defined with a total pressure of 58 kPa and a total temperature of 294 K. A static pressure was applied at the exit of the stator vane. Nonslip and adiabatic conditions were specified for all walls, and a scalable wall function was applied to determine the velocities at the nodes near the wall. Transient rotor stator interface models were used at the interfaces of adjacent blade rows. During the unsteady simulation, a series of numerical probes were arranged in the circumferential and span

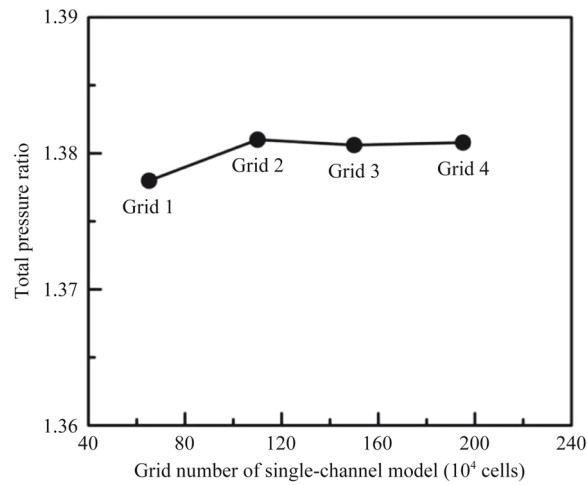


**Fig. 3** Variations of the total pressure ratio with different grid numbers at the design point

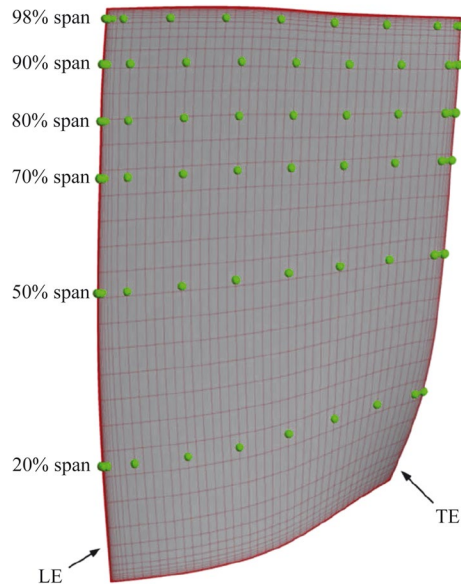


**Fig. 4** Distribution of numerical probes on the rotor blade

directions to obtain time-domain pressure signals, and the position distributions of the numerical probes are shown in Fig. 4.

### 3 Results and discussions

#### 3.1 Compressor performance and validation

To investigate the non-synchronous aerodynamic excitation of the unstable flow induced by high aerodynamic loading, the compressor operates under high aerodynamic loading conditions, and the angle adjustment of the S1 variable vane in the present study were closed 8° relative to the design condition. The comparisons of the inlet flow angles are shown in Fig. 5, where the inlet flow angles are based on the axial direction. The

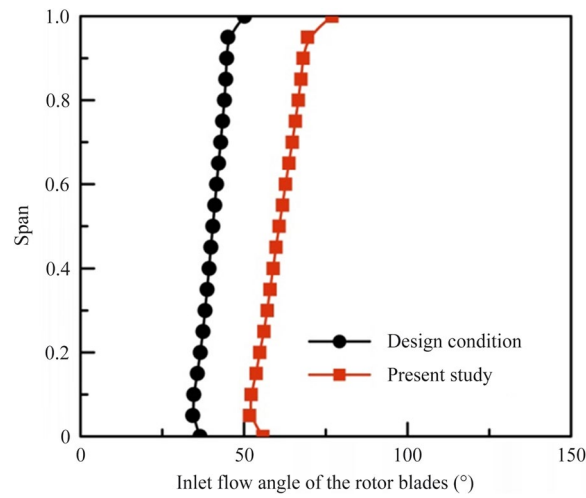


**Fig. 5** Comparison of inlet flow angle of the rotor blades

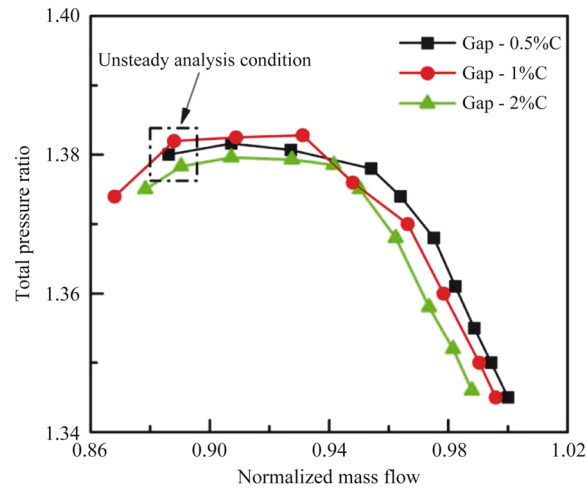


**Fig. 6** Characteristic curve of the compressor total pressure ratio

aerodynamic loading of the first-stage rotor increased with an increase in the inlet flow angle, and the tip region increased more than that of the root region.

Single passage steady simulations were conducted to obtain the stability boundary of the 1-1/2 stage compressor, and full-annulus unsteady simulations were performed under near stall conditions. During the experiment, the first-stage rotor blades exhibited the NSV phenomenon at the 90% speed off-design condition, and the numerical simulation in this study was conducted for the 90% speed condition. The numerical simulations were performed using the commercial CFD code. The comparison of the aerodynamic characteristic curve (total pressure ratio vs. normalized mass flow) under different tip clearances is shown in Fig. 6, where three typical tip clearances of 0.5%C, 1%C, and 2%C were selected to study the effect of tip clearance on the overall performance of the compressor. The abscissa is a dimensionless mass flow using the choked mass flow under the design condition. As the tip clearance increases, the total pressure

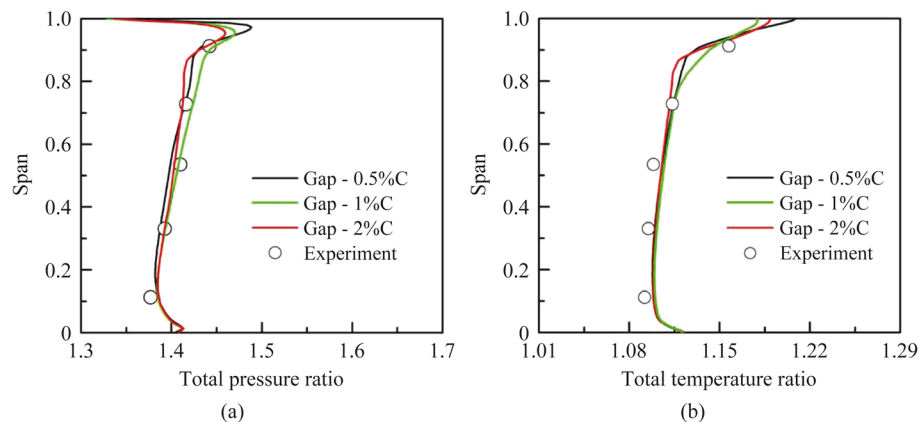
ratio and the normalized mass flow parameters first increase and then decrease under high aerodynamic loading conditions instead of constantly decreasing.

Figure 7 shows a comparison of the span direction distributions of the total pressure ratio and total temperature ratio of the rotor blade outlet under near stall conditions. The experiment interstage parameters are obtained by the S1 vane sensing area of the leading edge locations, and the tip clearances of rotor blades are obtained through three capacitive sensors on the casing wall. The tip clearance variation affects the pressure ratio distribution from the 50% span to the tip region, and the aerodynamic parameter changes most intensely at the tip region. Overall, the radial distribution of the aerodynamic parameters in the numerical simulation matches well with the experimental results, demonstrating that the effectiveness and accuracy of the numerical simulations have a good ability to capture the internal flow field of the rotor tip region. In summary, this numerical method could be used in subsequent investigations.

### 3.2 Non-synchronous aerodynamic excitation frequencies

Static pressure signals were obtained for the frequency spectral analysis of the numerical probes mounted on the rotor blade surface. The normalized static pressures at a 98% span of the rotor leading edge are shown in Fig. 8. For the 0.5%C tip clearance, the pressure fluctuation amplitude is significantly larger than those of both 1%C and 2%C tip clearances at near stall conditions, with an amplitude of approximately 19%. Furthermore, as the tip clearance increases to 1%C, the amplitude of the pressure fluctuation rapidly decreases to 6%. The pressure fluctuation amplitude for the 2%C tip clearance is slightly larger than that of the 1%C tip clearance. This indicates that distinct types of flow structures exist in the tip region under different tip clearances and high aerodynamic loadings under near stall conditions.

The frequency spectra in the rotating frame obtained by the Fast Fourier Transform (FFT) of the monitored static pressure on the 98% span leading edge are shown in Fig. 9. Non-synchronous aerodynamic excitation frequencies were observed throughout the full-annulus unsteady simulation. For the 0.5%C tip clearance, it can be seen that there is a very low non-synchronous aerodynamic excitation frequency (1.36 EO)



**Fig. 7** Comparison of aerodynamic parameters of the rotor blade outlet along the radial direction at near stall conditions. **a** Total pressure ratio. **b** Total temperature ratio

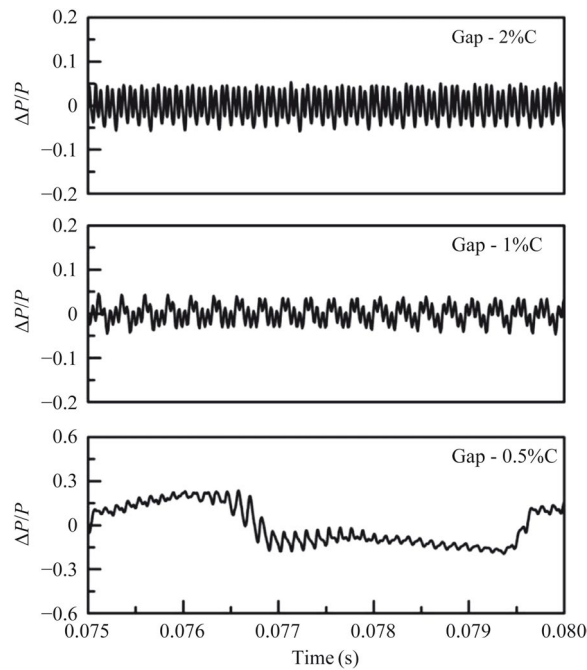


**Fig. 8** Monitored pressure in the rotating frame at 98% span leading edge position

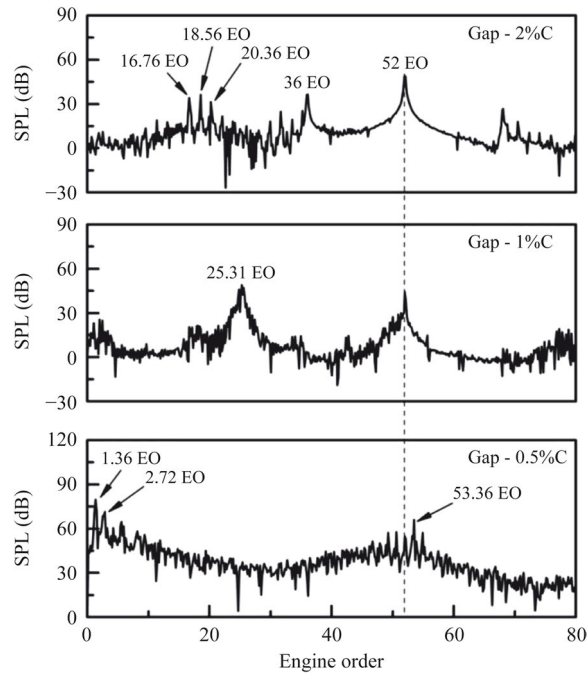


**Fig. 9** Frequency spectra of monitored static pressure in the rotating frame

and its harmonic frequency (2.72 EO), which are not harmonic with the rotating frequency. The non-synchronous aerodynamic excitation frequencies may cause NSV problems in the rotor blades owing to the high-amplitude pressure oscillation. For the 1%C and 2%C tip clearances, the aerodynamic excitation frequencies of 25.31 EO



and 18.56 EO exhibited an obvious broadband hump characteristic, which are also characterized by a non integral multiple of the rotating frequency. The frequencies of the broadband hump were roughly centered in the 40% – 60% range of the rotor blade passing frequency. This frequency spectrum has been reported by several researchers to be a rotating instability phenomenon [21–25].

A Spatial Fast Fourier Transform (SFFT) was used to obtain the circumferential mode order of non-synchronous aerodynamic disturbances. The SFFT was performed on circumferential pressure signals at different spans of leading edge locations: 20%, 50%, 80%, and 98% spans, respectively. A total of 2048 sampling points in the circumferential direction were used to improve the accuracy of the circumferential mode order, as shown in Fig. 10. For the 0.5%C tip clearance, the circumferential dominant mode order was 19 for different span positions, and the mode amplitude in the tip region was significantly higher than that of the blade root location. This indicates that the non-synchronous aerodynamic excitation was mainly generated by the instability of the tip flow. The mode order of the disturbance was approximately the rotor blade-passing number, and 66 mode orders were combined with the addition of frequencies between 19 and 47. The amplitude of the 19 main mode orders decreased as the tip clearance increased to 1%C.

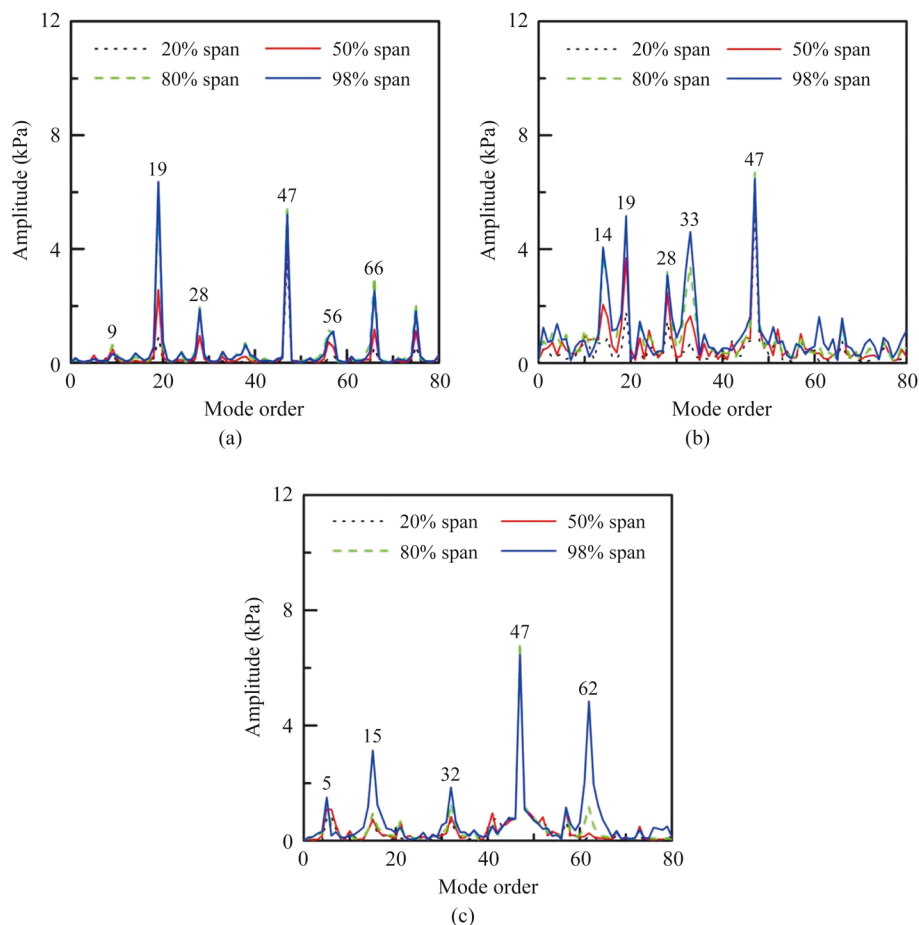


**Fig. 10** Circumferential mode number of aerodynamic disturbance under different tip clearances. **a** 0.5%C tip clearance. **b** 1%C tip clearance. **c** 2%C tip clearance

For the 2.0%C tip clearance, the circumferential dominant mode number of the aerodynamic disturbance was 47 for different span locations. The comparison of the SFFT results for different span locations indicated that the tip region was closer to the non-synchronous propagating flow disturbance source in the flow field.

### 3.3 Flow structure and instabilities

The relative Mach number distribution at the rotor exits clearly indicates the aerodynamic circumferential mode order under different tip clearances, as shown in Fig. 11. For the 0.5%C tip clearance, the aerodynamic circumferential mode order was 19, and there were 19 unstable flow structures in the circumferential direction. For the 1%C and 2%C tip clearances, the amplitude of the unstable flow structure was relatively lower. The low Mach number region in the circumferential direction is mainly caused by the trailing edge tip leakage flows. The circumferential dominant mode order was 47.

Figure 12 shows the relative Mach number in one annulus at the 98% span of the rotor for different tip clearances.  $\Delta P$  is the differential pressure between the transient pressure and the circumferential average value at the 98% span leading edge location of the rotor blade. As for high aerodynamic loading, the annular cascade results indicate that the unsteady vortices originate from the boundary layer separation under 0.5%C tip clearance at near stall conditions. The circumferential oscillation of separation vortices exhibits periodic shedding and reattachment processes on the suction side, and the periodic shedding and reattachment processes of rotor blades separated by 2 – 3 pitches result in 19 dominant mode orders in the circumferential direction. For the 1%C and 2%C tip clearances, the difference of tip flow structures in each blade passage is significantly weakened, which resulted in 47 dominant mode orders in the circumferential direction. The instability of the tip flow was mainly caused by the tip leakage flow, and the pressure fluctuation is significantly weaker than that of the 0.5%C tip clearance case. This indicates that the pressure fluctuation caused by the separation flow is much stronger than the tip leakage flow. The tip leakage flow passes over multiple tip clearance passages, and as a result, the unstable flow can propagate in the circumferential direction. As the tip clearance increases, the circumferential propagation of the tip leakage flow suppresses the blockage at the tip region, thereby suppressing the separation of the boundary layer on the suction surface. As the tip clearance increases further, the unstable flow intensity and losses caused by the tip leakage flow increase.

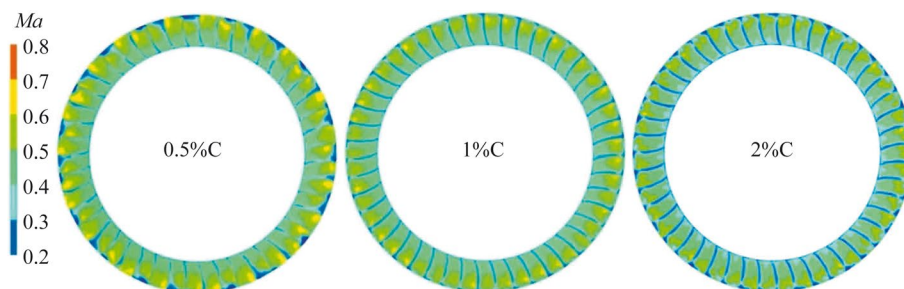


**Fig. 11** Relative Mach number distribution at the rotor exits under different tip clearances

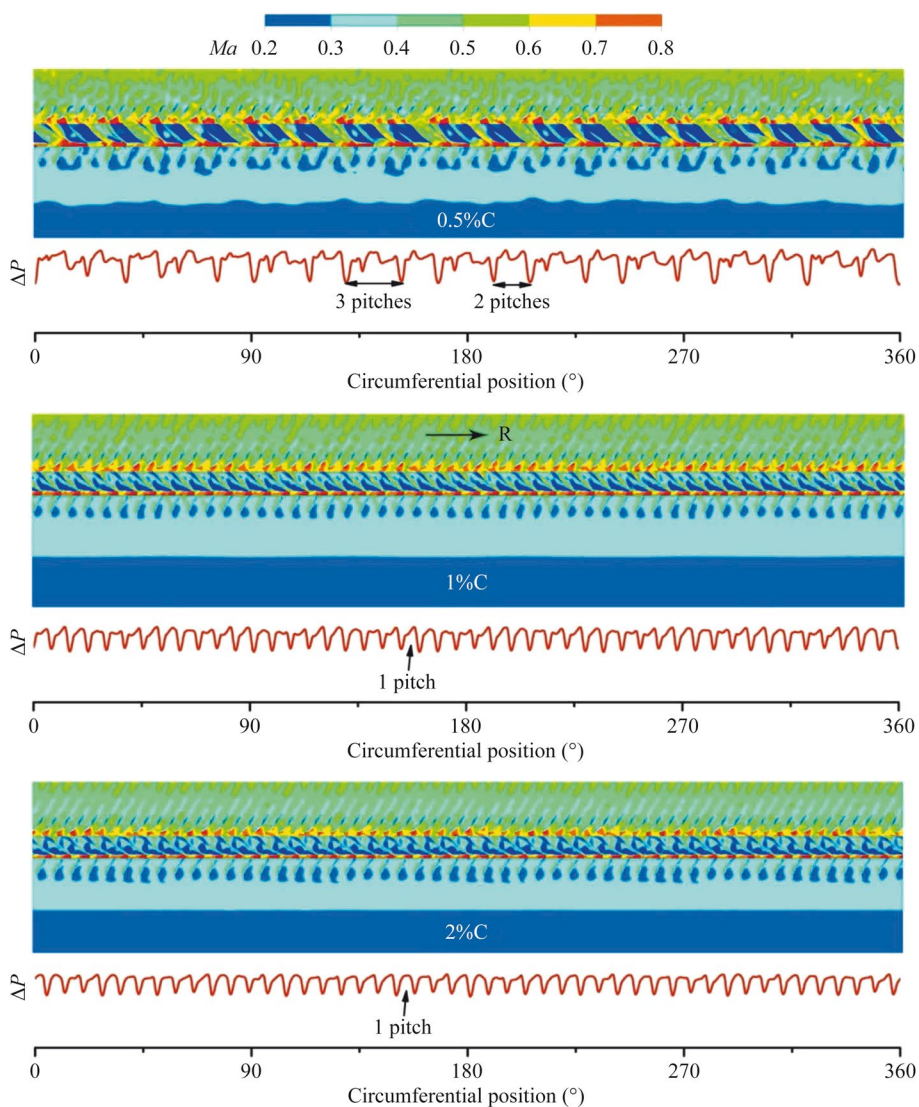


**Fig. 12** Relative Mach number in one annulus at the 98% span of the rotor under different tip clearances

Figure 13 shows the unstable flow structure near the rotor tip region under different tip clearances, where the streamlines start from the rotor tip clearance. For the 0.5%*C* tip clearance, 19 unstable flow structures were clearly visible in the circumferential direction, which is consistent with the circumferential mode number in Fig. 10a. A large-scale oscillating vortex is a tornado-like separation vortex, and the circumferential propagation mechanism of large-scale tornado-like separation vortices is similar to the classical explanation of a spike stall cell [26–28]. The separation of multiple blades in the circumferential direction led to higher mode-order disturbances. Tornado-like separation vortices also exist for a tip clearance of 1%*C*, but their spatial size and intensity seem to be significantly weakened compared with the 0.5%*C* tip clearance case. Simultaneously, the intensity of the tip leakage flow is significantly enhanced as the tip clearance increases. For a large tip clearance of 2%*C*, there were no tornado-like separation vortices in the tip region, and the tip flow states in each

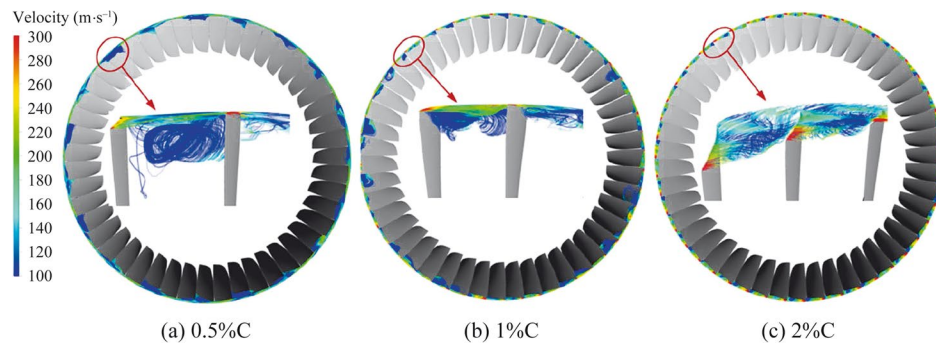


**Fig. 13** Unstable flow structure near the rotor tip region under different tip clearances

passage were similar. The tip leakage flows can pass over multiple tip clearances and form the leading edge vortex and the tip leakage vortex. The leading edge tip vortex impinged on the pressure side of the adjacent blades. The leakage flows from the middle and rear parts interact with the mainstream fluid and flows out of the blade passage. As the tip clearance increases, the impingement location of the leading edge tip vortex moves forward and the leakage flow is enhanced to cross the tip clearance of the adjacent blades. Qualitatively, as the tip clearance increases, the fluid can pass through the tip clearance to the suction side, which increases the local radial pressure gradient and suppresses boundary layer separation on the suction surface. The scale of the tornado-like separation vortices was significantly larger than that of the tip leakage vortex, resulting in a large amount of low energy fluid and high amplitude pressure fluctuations.

#### 4 Conclusion

We presented a numerical study of the non-synchronous propagating flow disturbances of a compressor rotor with high aerodynamic loading. Time-accurate computations were conducted under near stall conditions for three typical tip clearances. The non-synchronous aerodynamic excitation frequency, the circumferential mode characteristics, and the annular unstable flow structures were analyzed, and the following conclusions were drawn.

1. For high aerodynamic loading, the total pressure ratio first increases and then decreases as the tip clearance increases, and the choke flow decreases when the tip gap increases. The boundary layer growth and separation results in a loss increment for the 0.5%C tip clearance case.
2. Tip clearance has a significant effect on the pressure fluctuation amplitude and the non-synchronous aerodynamic excitation frequency. For the 0.5%C tip clearance case, the circumferential oscillation of unsteady vortices exhibits periodic shedding and reattachment processes. The traveling large-scale tornado-like separation vortices cause low non-synchronous aerodynamic excitation frequency and severe pressure fluctuations. The periodic shedding and reattachment processes of the rotor blades separated by 2 – 3 pitches result in 19 dominant main mode orders in the circumferential direction.

- As the tip clearance increased from 1%C to 2%C, the cross-channel propagation of the tip leakage flow increased the local radial pressure gradient and suppressed the boundary layer separation on the suction surface. The difference of tip flow structures in each blade passage was significantly weakened, and the dominant mode order of the disturbance was equal to the rotor blade-passing number. Furthermore, the pressure fluctuation were mainly caused by the cross-channel tip leakage flow, and the aerodynamic excitation frequency exhibited evident broadband hump characteristics, which has been reported as a rotating instability phenomenon.

#### Acknowledgements

We would like to thank reviewers for taking the time and effort necessary to review the manuscript. We sincerely appreciate all valuable comments and suggestions, which helped us to improve the quality of the manuscript.

#### Authors' contributions

Songbai Wang: Methodology, Software, Formal analysis, Data curation, Writing - Original draft preparation, Funding acquisition. Yong Chen: Review and Editing. Yadong Wu: Review and Editing. All authors read and approved the final manuscript.

#### Funding

This work is supported by the National Science and Technology Major Project (J2022-IV-0010-0024).

#### Availability of data and materials

The data that support the findings of this study are available from the corresponding author upon reasonable request.

#### Declarations

##### Competing interests

The authors do not have any competing interests.

Received: 8 January 2024 Accepted: 31 March 2024

Published online: 04 July 2024

#### References

- Neuhaus L, Schulz J, Neise W et al (2003) Active control of the aerodynamic performance and tonal noise of axial turbomachines. *Proc Inst Mech Eng A J Power Energy* 217(4):375–383
- Han L, Wei DS, Wang YR et al (2021) Analysis method of nonsynchronous vibration and influence of tip clearance flow instabilities on nonsynchronous vibration in an axial transonic compressor rotor. *J Turbomach* 143(11):111014
- Zhu X, Hu P, Lin T et al (2022) Numerical investigations on non-synchronous vibration and frequency lock-in of low-pressure steam turbine last stage. *Proc Inst Mech Eng A J Power Energy* 236(4):647–661
- Baumgartner M, Kameier F, Hourmouziadis J (1995) Non-engine order blade vibration in a high pressure compressor. In: Proceedings of the twelfth international symposium on airbreathing engines. Melbourne, September 1995
- Kielb RE, Barter JW, Thomas JP et al (2003) Blade excitation by aerodynamic instabilities: a compressor blade study. In: Proceedings of the ASME turbo expo 2003, collocated with the 2003 international joint power generation conference. Atlanta, 16-19 June 2003
- Vo HD (2010) Role of tip clearance flow in rotating instabilities and nonsynchronous vibrations. *J Propul Power* 26(3):556–561
- Yang F, Wu YH (2021) The tip leakage vortex breakdown and its possible relationship with rotating instability in a subsonic compressor rotor. In: Proceedings of the ASME turbo expo 2021: turbomachinery technical conference and exposition. Online, 7-11 June 2021
- Mailach R, Lehmann I, Vogeler K (2008) Periodical unsteady flow with a rotor blade row of an axial compressor-part I: flow field at midspan. *J Turbomach* 130:041004
- Mailach R, Sauer H, Vogeler K (2001) The periodical interaction of the tip clearance flow in the blade rows of axial compressors. In: Proceedings of ASME Turbo Expo 2001. Volume 1: turbomachinery. New Orleans, 4-7 June 2001
- Mailach R, Lehmann I, Vogeler K (2001) Rotating instabilities in an axial compressor originating from the fluctuating blade tip vortex. *J Turbomach* 123(3):453–460
- Im HS, Zha GC (2014) Investigation of flow instability mechanism causing compressor rotor-blade non-synchronous vibration. *AIAA J* 52(9):2019–2031
- Im HS, Zha GC (2014) Investigation of non-synchronous vibration mechanism for a high-speed axial compressor using delayed DES. In: Proceedings of the 52nd aerospace sciences meeting. National Harbor, 13-17 January 2014
- Wu YD, Li T, Lai SZ et al (2021) Investigation of rotating instability characteristics in an axial compressor with different tip clearances. *Proc Inst Mech Eng G J Aerosp Eng* 235(15):2225–2239
- Peng C (2011) Tip running clearances effects on tip vortices induced axial compressor rotor flutter. In: Proceedings of the ASME 2011 turbo expo: turbine technical conference and exposition. Vancouver, 6-10 June 2011

15. Jüngst M, Holzinger F, Schiffer HP et al (2015) Analysing non-synchronous blade vibration in a transonic compressor rotor. In: Proceedings of 11th European conference on turbomachinery fluid dynamics & thermodynamics. Madrid, 23-27 March 2015
16. Han L, Wei DS, Wang YR et al (2022) Lock-in phenomenon of tip clearance flow and its influence on aerodynamic damping under specified vibration on an axial transonic compressor rotor. *Chinese J Aeronaut* 35(3):185–200
17. Han L, Wei DS, Wang YR et al (2020) Locked-in phenomenon between tip clearance flow instabilities and enforced blade motion in axial transonic compressor rotors. In: Proceedings of the ASME turbo expo 2020: turbomachinery technical conference and exposition. Online, 21-25 September 2020
18. Drolet M, Vo HD, Mureithi NW (2011) Effect of tip clearance on the prediction of non-synchronous vibrations in axial compressors. In: Proceedings of the ASME 2011 turbo expo: turbine technical conference and exposition. Vancouver, 6–10 June 2011
19. Wu Y, An G, Chen Z et al (2016) Origins and structure of rotating instability: part 2 — Numerical observations in a transonic axial compressor rotor. In: Proceedings of the ASME turbo expo 2016: turbomachinery technical conference and exposition. Seoul, 13-17 June 2016
20. Du J, Li JC, Wang K et al (2013) The self-induced unsteadiness of tip leakage flow in an axial low-speed compressor with single circumferential casing groove. *J Therm Sci* 22(6):565–572
21. Wang H, Wu YD, Ouyang H et al (2016) Circumferential propagating characteristics of tip leakage flow oscillation and its induced rotating pressure wave. *Proc Inst Mech Eng A J Power Energy* 230(4):374–387
22. Wu Y, Li Q, Chu W et al (2010) Numerical investigation of the unsteady behaviour of tip clearance flow and its possible link to stall inception. *Proc Inst Mech Eng A J Power Energy* 224(1):85–96
23. Yang ZY, Wu YD, Liu ZL et al (2023) Tip flow on rotating instability on an axial compressor with different tip clearances. *Aerosp Sci Technol* 139:108364
24. Li T, Wu YD, Ouyang H (2021) Numerical investigation of tip clearance effects on rotating instability of a low-speed compressor. *Aerosp Sci Technol* 111:106540
25. Pardowitz B, Moreau A, Tapken U et al (2015) Experimental identification of rotating instability of an axial fan with shrouded rotor. *Proc Inst Mech Eng A J Power Energy* 229(5):520–528
26. Deppe A, Saathoff H, Stark U (2005) Spike-type stall inception in axial-flow compressors. In: Proceedings of the 6th European conference on turbomachinery - Fluid dynamics and thermodynamics. Lille, 7-11 March 2005
27. Vo HD, Tan CS, Greitzer EM (2005) Criteria for spike initiated rotating stall. In: Proceedings of the ASME turbo expo 2005. Reno, 6-9 June 2005
28. Möller D, Schiffer HP (2021) On the mechanism of spike stall inception and near stall nonsynchronous vibration in an axial compressor. *J Eng Gas Turbines Power* 143(2):021007

### **Publisher's Note**

Springer Nature remains neutral with regard to jurisdictional claims in published maps and institutional affiliations.